

## Direct Electron Transfer Response of Superoxide Dismutase on a Graphene-Based Modified Electrode

Jie Jiang<sup>1,2</sup>, Miao-Qing Xu<sup>1</sup>, Guang-Chao Zhao<sup>1,\*</sup>

<sup>1</sup>College of Environmental Science and Engineering, Anhui Normal University, Wuhu, 241000, P R China

<sup>2</sup>Chuzhou Vocational and Technical College, Chuzhou, 239000, P R China

\*E-mail: [gczhao@mail.ahnu.edu.cn](mailto:gczhao@mail.ahnu.edu.cn)

Received: 4 January 2015 / Accepted: 26 January 2015 / Published: 24 February 2015

---

Single stranded DNA (ssDNA)/graphene (GR) nanocomposites were prepared by a chemical route and cast on basal plane graphite (BPG) electrode to construct an ssDNA/GR modified electrode. Copper-zinc superoxide dismutase (SOD) was adsorbed tightly on the surface of the modified electrode and the direct electron transfer of SOD was investigated using cyclic voltammetry. A couple of well-defined and quasi-reversible CV peaks of SOD can be observed and the separation of anodic and cathodic peak potentials is 90 mV in a phosphate buffer solution (pH 7.0). The electron transfer rate constant ( $k_s$ ) of SOD is  $1.45 \text{ s}^{-1}$ . Furthermore, this biosensor exhibits high analytical performance with a wide linear range (0.05–0.45  $\mu\text{M}$ ), low detection limit (3 nM) and fast response time (1.5 s). The results demonstrate that the ssDNA-graphene nanocomposite offers a biocompatible material for the construction of biofuel cells, bioelectronics and biosensors.

---

**Keywords:** Graphene, Superoxide dismutase, Direct electron transfer, Biosensor

### 1. INTRODUCTION

Superoxide dismutase (SOD) has been known to be ubiquitously distributed in aerobic organisms and to play an important role in cell protection mechanisms against oxidative damage from reactive oxygen species [1] by specifically catalyzing the dismutation of the superoxide anion ( $\text{O}_2^-$ ) to  $\text{O}_2$  and  $\text{H}_2\text{O}_2$ . Therefore, electron transfer of SOD has been attracting more attention due to its importance in the understanding of the intrinsic thermodynamic and kinetic properties of SOD, more importantly, in the practical development of third-generation biosensors for  $\text{O}_2^-$ , which is concerned with traumatic brain injury, ischemia-reperfusion, and hypoxia. Unfortunately, the active-site Cu (II)/Cu (I) ion is at the bottom of a deep channel on the outside of the  $\beta$ -barrel between two large loops.

The channel is narrow width ( $<4 \text{ \AA}$ ), and the Zn (II) is completely buried [2], which would prohibit the electrical communication between the protein and normal electrode surface. Immobilizing SOD on the promotor-modified electrode was proven to be the main path to probe the electron transfer of SOD. For instance, Ohsaka's group found that the facilitated electron transfer of the SOD could be observed when the SOD molecule is confined on a thiol (e.g., cysteine) self-assembled monolayer (SAM) on the Au substrate [3]. Recently, a reversible redox response of Cu/Zn-SOD has been observed at an Hg electrode, carbon nanotube (CNT)-modified electrode, and in silica sol-gel film [4-8]. Up to today, the interaction between promoter and SOD is still a vital topic of investigation.

Graphene, a single-atom-thick and two-dimensional carbon material, has been triggered enormous interest because of its remarkable electronic, mechanical and thermal properties. Due to their unique nanostructure and extraordinary properties, graphene-based materials are attractive as nanoscale building block for the synthesis of graphene-based composites [9-11], which have potential applications in gas sensors, pH sensors and optics [12-15]. Their subtle electronic properties suggest that graphene have the ability to promote electron transfer reactions when used as electrode materials in electrochemical reactions.

However, the requirement to obtain graphene as individual sheets and maintain it in the reduced form is a key challenge in the synthesis and processing of bulk-quantity graphene owing to the high cohesive van der Waals energy ( $5.9 \text{ kJ mol}^{-1}$  carbon) [16] adhering graphitic sheets to one another. Up to now, graphene can be fabricated by various effective ways. Among them, a simple way has been improved to prepare graphene in aqueous solution, in which graphene with the nature of a single flake was obtained by chemically reducing graphene oxide. In those methods, water-soluble polymers, such as polyvinylpyrrolidone,  $\alpha$ -MnO<sub>2</sub>, ZnO, polyaniline, polypyrrole were used as disperser to surmount the strong exfoliation energy of the  $\pi$ -stacked layers in graphene. The as-prepared graphene-based material had been utilized successfully to construct electrochemical sensing and biosensing platform [17-20].

DNA is an important biological macromolecule that acts as a form of memory storage for genetic information. Meanwhile, Owing to the potential of interaction between the nitrogenous bases of DNA with other biomolecules in life science, considerable attention has been paid on electrochemical DNA biosensor in the diagnosis of genetic diseases and the detection of pathogenic biological species [21]. On the other hand, Stephen and co-works have demonstrated that graphene can be successfully functionalized using single-stranded(ss) DNA to produce stable aqueous suspensions of graphene single sheets with concentrations as high as  $2.5 \text{ mg mL}^{-1}$ , and this novel nanocomposites may have potential applications in bionanotechnology [22].

In the present report, we employed a related approach to fabrication of ssDNA-dispersed graphene nanocomposites. Then ssDNA-dispersed graphene was immobilized on the surface of basal plane graphite electrode to form an ssDNA/GR modified electrode. The direct electron transfer and electrocatalytic performance of superoxide dismutase (SOD) was achieved at this modified electrode.

## 2. EXPERIMENTAL

### 2.1 Apparatus and reagents

Electrochemical experiments were performed with CHI660 electrochemical analyzer (CHI, USA) with a conventional three-electrode cell. The SOD/ssDNA-GR modified BPG electrode (5.2 mm diameter) was used as a working electrode. An Ag/AgCl electrode and a platinum wire electrode were used as the reference and the auxiliary electrodes, respectively.

Copper-zinc superoxide dismutase (SOD) was from Toyobo. It was used as received without further purification. SOD solution ( $1.5 \text{ mg mL}^{-1}$ ) was stored at a temperature of  $4 \text{ }^{\circ}\text{C}$  as stock solution. DNA Fish Sperm, Sodium salt was purchased from Biodee Company. The molecular weight (MW) is not determined by Biodee. DNA solution ( $8 \text{ mg mL}^{-1}$ ) was stored at a temperature of  $4 \text{ }^{\circ}\text{C}$ . Other chemicals were of analytical grade and used without further purification. All solutions were made up with doubly distilled water and were deaerated with high purity nitrogen before performing the experiments and maintained under nitrogen atmosphere during measurements.

### 2.2 Procedures

#### 2.2.1 Preparation of ssDNA-stabilized graphene dispersion

Graphene oxide (GO) was prepared from graphite according to the Hummers-Offeman method [23]. The obtained graphene oxide was washed with deionized water six times to remove the remaining metal ions and acid. Then, the product was dried under vacuum and stored for use. Single stranded DNA (ssDNA) was produced by heating a DNA solution ( $8 \text{ mg mL}^{-1}$ ) in an oil bath ( $100 \text{ }^{\circ}\text{C}$ , 5 min) followed by rapid cooling in an ice bath. After that, 2 mL ssDNA was added into GO solution (2 mL,  $1 \text{ mg mL}^{-1}$ ) and subsequently mixed by ultrasonication for 30 min to form a lightly yellow dispersion. Hydrazine hydrate solution (20  $\mu\text{L}$ ) was added to the lightly yellow solution. The resultant mixture was stirred for 5 min and reacted at  $100 \text{ }^{\circ}\text{C}$  for 18 hours. The color of mixture solution changed from lightly yellow to black after the end of the reaction, indicating the reduction of graphene oxide. The ssDNA/graphene dispersion stored in refrigerator (*temperature*  $4 \text{ }^{\circ}\text{C}$ ).

#### 2.2.2 Electrode preparation

Prior to the modification, the BPG electrode was polished with abrasive paper before each experiment and then washed with double distilled water and ethanol in an ultrasonic bath successively.

After carefully washed with water, the BPG electrode was treated by dropping 5  $\mu\text{L}$  of ssDNA-stabilized graphene suspension and then dried in air. The resultant electrode was soaked in double distilled water for 3 h and again rinsed with water to remove unadsorbed ssDNA-dispersed graphene. Thus, an ssDNA-dispersed graphene modified basal plane electrode was obtained and denoted as ssDNA-GR/BPG electrode. Subsequently, the ssDNA-GR/BPG electrode was incubated in phosphate

buffer solution (pH 7.0) containing Cu/Zn-SOD ( $1.5 \text{ mg mL}^{-1}$ ) for 20 min, and immediately rinsed with water to remove any unbound Cu/Zn-SOD. It was denoted as SOD/ssDNA-GR/BPG electrode.

In order to comparison, the SOD/GR modified electrode without ssDNA, the SOD/ssDNA modified electrode without graphene and the SOD/BPG modified electrode without ssDNA-GR were also constructed in the same way only omitting the addition of ssDNA, graphene or ssDNA-stabilized graphene, respectively.

### 3. RESULTS AND DISCUSSION

#### 3.1 Direct electrochemistry of SOD on ssDNA-GR/BPG electrode

The metal active-site of SOD ( $\text{Cu}^{2+}/\text{Zn}^{2+}$  in oxidized form) is structurally located deep in a channel with narrow width ( $<4 \text{ \AA}$ ), which blocks the direct electron transfer between the enzyme and the electrodes. Nevertheless, we have realized the direct electron transfer of SOD at the ssDNA-GR modified electrode. Fig.1 displays typical cyclic voltammograms (CVs) obtained at different SOD-modified electrodes in  $\text{N}_2$ -saturated protein-free phosphate buffer solution (50 mM, pH 7.0). A pair of well-defined and nearly reversible oxidation-reduction peaks was observed (Fig. 1c) at the SOD/ssDNA-GR modified electrode and the separation of anodic and cathodic peak potentials ( $\Delta E_p$ ) is 90 mV. The redox response was not observed at the ssDNA-GR modified electrode in the same solution (date not show here). This result demonstrates that the observed redox response is ascribable to the SOD bound on the surface of ssDNA-GR modified electrode. This fact also points out a favorable adsorption orientation of SOD at the ssDNA-GR electrode surface, in which the negatively charged graphene sheets are thought to provide suitable attractive adsorption sites leading to a facilitated direct electron transfer of the positively charged redox protein, SOD.

SOD/GR modified electrode (curve b in Fig. 1) also displays a couple of redox peaks of SOD. However, these redox peak currents are much smaller than those measured on the SOD/ssDNA-GR modified electrode. A plausible explanation for the observed behavior could be given by taking into account the electrode materials with a terminal group of  $-\text{COOH}$  well promote the direct electron-transfer of Cu/Zn-SOD [3], while those with terminal groups of  $-\text{NH}_2$ ,  $-\text{CH}_3$ ,  $-\text{SO}_3^-$  or  $-\text{OH}$  do not. In our electrode system, chemically reduced graphene oxide also contains a few carboxylic groups which uniformly distributed on the GO surface with no selectivity. So, the exact nature of this promoter effect is due to the residual carboxylic groups distributed on the chemically reduced graphene surface. As to the SOD/ssDNA modified electrode, it displays a smaller redox peak and lower background current. A hydrosoluble promoter like ssDNA may leach out of the electrode and therefore cannot offer a suitable biocompatible microenvironment for protein, which may lead to significant signal loss and affect the stability of the biosensor. In this case, graphene used here serves dual purpose for providing sufficient steric hindrance to keep the ssDNA stable and also for use as electron conductor due to their subtle electronic properties. This phenomenon provides an evidence for the successful confinement of the SOD at the SOD/ssDNA-GR modified electrode.

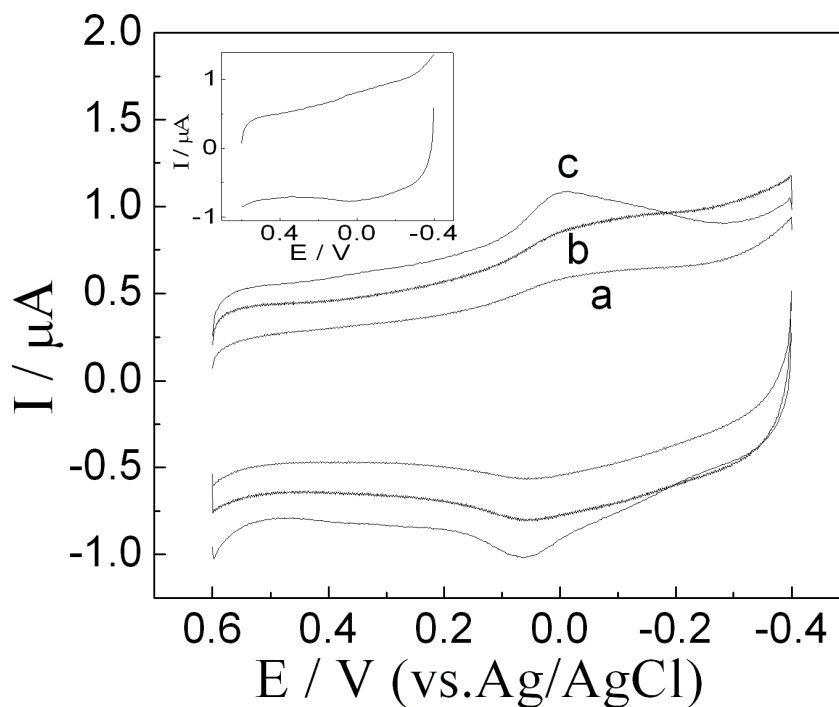


**Figure 1.** Cyclic voltammograms of SOD/ssDNA/BPG (a), SOD/GR/BPG (b) and SOD/ssDNA-GR/BPG(c) electrodes in pH 7.0 phosphate buffer solution. Inset: CV of the SOD/BPG electrode in pH 7.0 PBS. Scan rate:  $100 \text{ mV s}^{-1}$ .

In the fabrication process of the electrode, SOD was adsorbed on electrode surface through soaking ssDNA-GR modified electrode into SOD solution. So, optimum adsorption time of SOD was also investigated. Fig. 2 is a typical cyclic voltammogram (CV) for the adsorption process of SOD on the ssDNA-GR modified electrode surface. In phosphate buffer solution (50 mM pH 7.0), no peaks can be observed for ssDNA-GR/BPG electrode (Fig. 2a). However, a pair of quasi-reversible redox peaks could be observed once it was dipped into the SOD solution, indicating that SOD could be adsorbed on the surface of the ssDNA-GR modified electrode immediately (Fig. 2b). As showed in this figure, both anodic and cathodic peak currents increase with increasing the adsorption time. But when the adsorption time is more than 15 min, no dramatically change of the redox peaks currents can be observed, which means that the adsorption of SOD on the ssDNA-GR modified electrode surface reaches a saturated state (as shown in Fig. 2e).

The dependence of CV peak current on the scan rate is investigated in the range from 0.2 to  $0.6 \text{ Vs}^{-1}$  (data not show). The peak current linearly increased with the scan rate with a correlation coefficient of 0.9973, suggesting that the reaction is a surface-controlled process. On the other hand, the peak-to-peak separation also increased lightly with the increasing of scan rate. According to Laviron's equation [24], the electron transfer rate constant ( $k_s$ ) of SOD at the ssDNA-GR modified electrode can be estimated to be  $1.45 \text{ s}^{-1}$ . The  $k_s$  value is larger than that of SOD adsorbed on a nion-cysteine modified gold electrode ( $1.0 \pm 0.1 \text{ s}^{-1}$ ) and cysteine modified Au electrode ( $1.3 \text{ s}^{-1}$ ) [25,3], suggesting ssDNA-GR composite is an excellent promoter for the electron transfer between SOD and electrode.

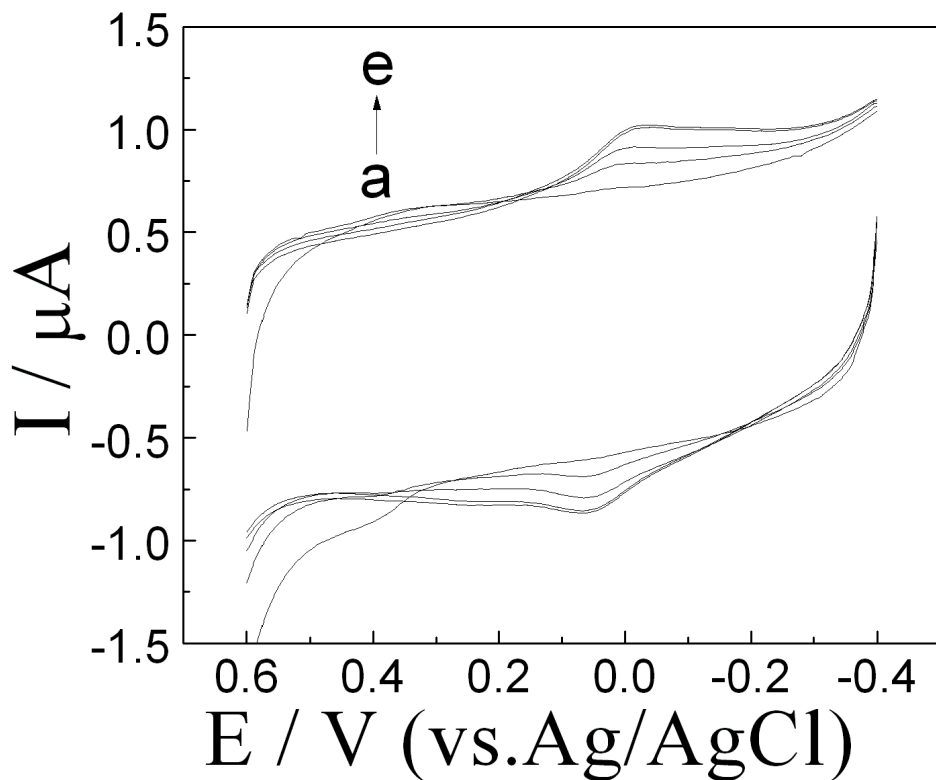


**Figure 2.** Cyclic voltammograms of SOD/ssDNA-GR modified BPG electrode based on different adsorption time of SOD (a) 0, (b) 2, (c) 6, (d) 15 and (e) 20min obtained in 0.1 M PBS (pH 7.0). Scan rate:  $100 \text{ mV s}^{-1}$ .

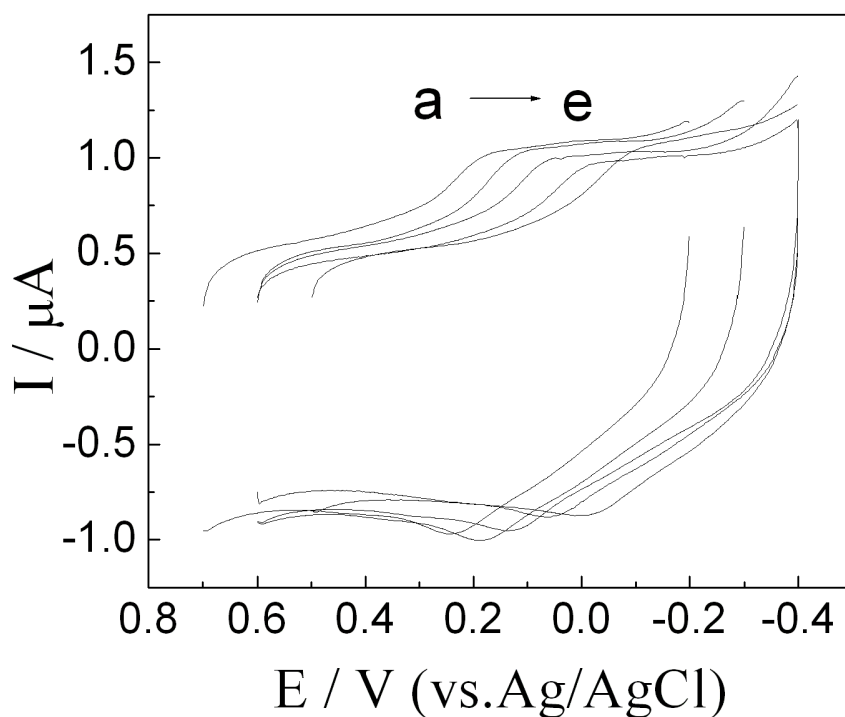


**Figure 3.** Cyclic voltammograms obtained at a SOD/ssDNA-GR/BPG modified electrode in different pH phosphate buffer solution. The pH values are 4, 5, 6, 7 and 9, respectively. Scan rate:  $100 \text{ mV s}^{-1}$ .

The influence of the acidity or alkalinity of the solution on the electro-activity of SOD at the ssDNA-GR composite surface was also examined in different pH buffer solutions (pH=4, 5, 6, 7, 8 and 9) via cyclic voltammetry (Fig.3). The apparent formal potential of the SOD Cu (II)/Cu (I) redox couple, which was estimated as the midpoint of cathodic and anodic peak potentials, had shifted linearly to the negative direction with the increase of pH value. The plot of formal potential versus pH showed a line with a slope of  $-53.9 \text{ mV pH}^{-1}$ , indicating one proton and one electron are involved in the electrode reaction of Cu/Zn-SOD, which is similar to the previously proposed scheme for the enzymatic catalytic mechanism of the Cu/Zn-SOD [26-28].

### 3.2 Electrocatalytic activity of SOD/ssDNA-GR/BPGE toward $\text{O}_2^-$

Experimental results demonstrated that the direct electron transfer of SOD was greatly facilitated at the ssDNA-GR composite surface. So it is desirable to clarify whether SOD retains its inherent biological activity after immobilized on the electrode surface.

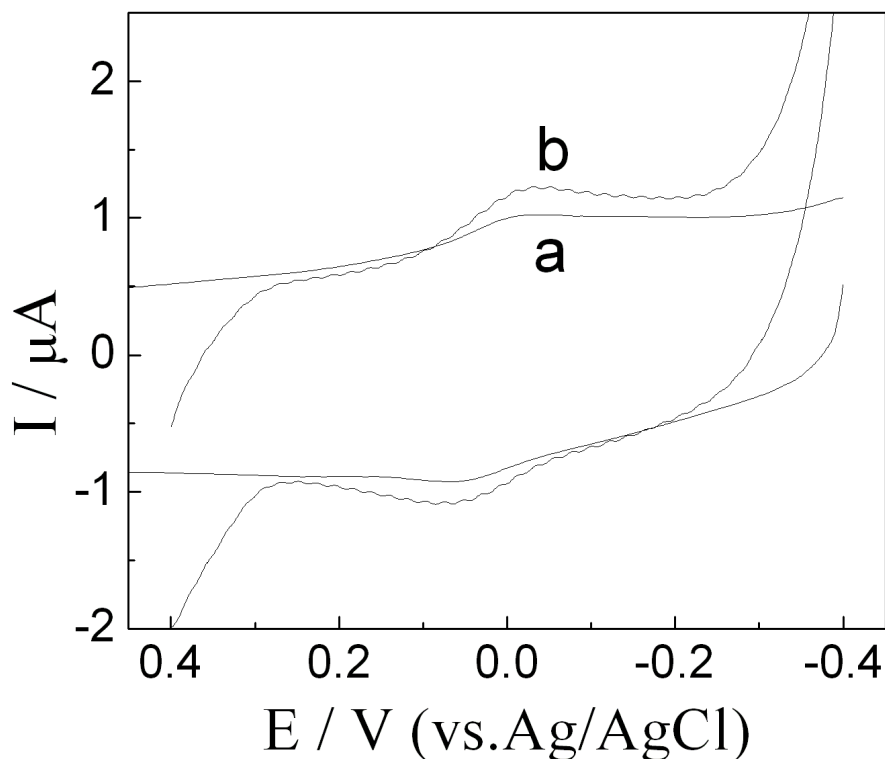


**Figure 4.** CVs obtained at (a) SOD/ssDNA-GR modified electrode in PBS, (b) SOD/ssDNA-GR modified electrode in PBS ( $\text{O}_2$ -saturated) containing 0.004 unit of XOD and 50  $\mu\text{M}$  xanthine. Scan rate:  $100 \text{ mV s}^{-1}$ .

The electrochemical response of the SOD/ssDNA-GR/BPGE resulted from  $\text{O}_2^-$  was investigated. A simple and efficient method was used for in situ generation of  $\text{O}_2^-$  based on the oxidation of xanthine to uric acid (UA) in the presence of xanthine oxidase (XOD) with 26% yield of

$O_2^-$  of the total xanthine. The measurement solution should be operated at a constant and high stirring speed (600 rpm) to acquire reproducible results. Fig. 4 displayed the CVs obtained at the Cu/Zn-SOD based electrode in the absence and presence of  $O_2^-$ .

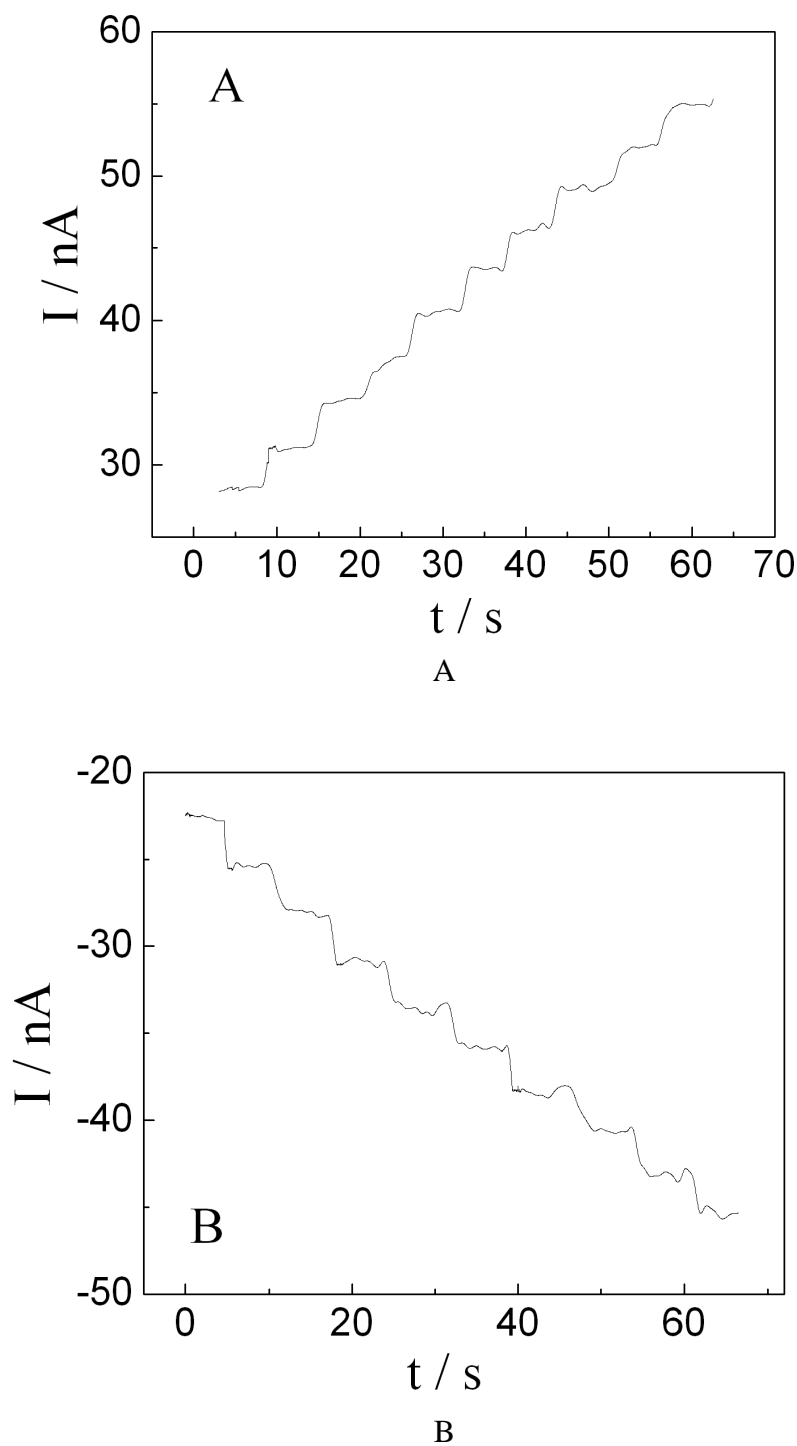
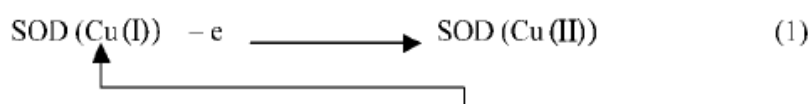


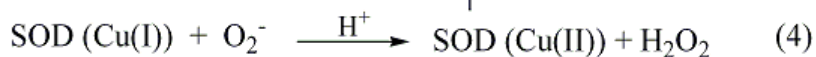
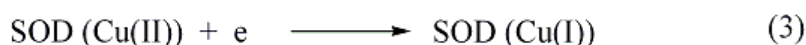
**Figure 5.** Amperometric responses of the SOD/ssDNA-GR/BPGE to successive 50 nM xanthine injection at applied potentials of  $-75\text{mV}$  (A) and  $100\text{mV}$  (B) in  $O_2$ -saturated 25mM PBS (pH 7.0) containing 0.004 unit of XOD and the stirring rate of solution is 600 rpm.



The activity of the SOD/ssDNA-GR/BPG electrode toward  $O_2^-$  was examined in 25 mM PBS ( $O_2$ -saturated) containing XOD (0.004 unit) and xanthine (50  $\mu$ M). As shown, both of the cathodic and anodic peak currents corresponding to the redox reaction of the SOD confined on the electrode are significantly increased, compared with those in the absence of  $O_2^-$ . The large anodic and cathodic currents starting from about 300 and -300 mV were due to the oxidation of uric acid (UA) and the reduction of  $H_2O_2$  and  $O_2$ , respectively.  $H_2O_2$  and UA are coproduced in the xanthine/XOD based  $O_2^-$ -generating system [29]. Such good bifunctional catalytic activity by SOD/ssDNA-GR/BPG is essentially based on the enzyme specificity of SOD for the dismutation of  $O_2^-$ ; i.e., SOD catalyzes both the reduction of  $O_2^-$  to  $H_2O_2$  and the oxidation to  $O_2$  via a redox cycle of its Cu/Zn complex moiety as well as the direct electron transfer of SOD. The following reaction mechanism can explain the enhanced oxidation current observed in the anodic scan:



Similarly, the reduction current is enhanced in the cathodic scan according to the following scheme:



Amperometric responses of SOD/ssDNA-GR/BPG electrode to successive concentration changes of  $O_2^-$  were conducted at the applied potential of 100 mV and -75 mV, and the corresponding current time responses are shown in Fig. 5. A side-step-like current response can be observed both at 100 mV and -75 mV; the currents increase stepwise with successive additions of xanthine (50 nM). The reductive current increases to reach a stable plateau within 1.5 s when adding xanthine into the buffer solution (25 mM). This suggested that the response of the electrode to  $O_2^-$  should be a quick responsive process.

In order to express clearly the relationship between response current and the concentration of xanthine, calibration plots of SOD/ssDNA-GR/BPG electrode with different xanthine concentrations (0.05–0.45  $\mu$ M) are shown in Fig. 6. It can be observed that the response currents change linearly with the xanthine concentration (0.05–0.45  $\mu$ M) both at -75 mV and 100 mV, with correlation coefficient of 0.99965 and 0.99912 respectively. The excellent detection limit ( $3\sigma$ ) of 3.00 nM was obtained at the applied potential of 100 mV (4.8 nM at the applied potential of -75 mV). The bifunctional enzymatic catalytic activity inherent in SOD substantially offers a potentially useful for flexible electrochemical determination of  $O_2^-$ .

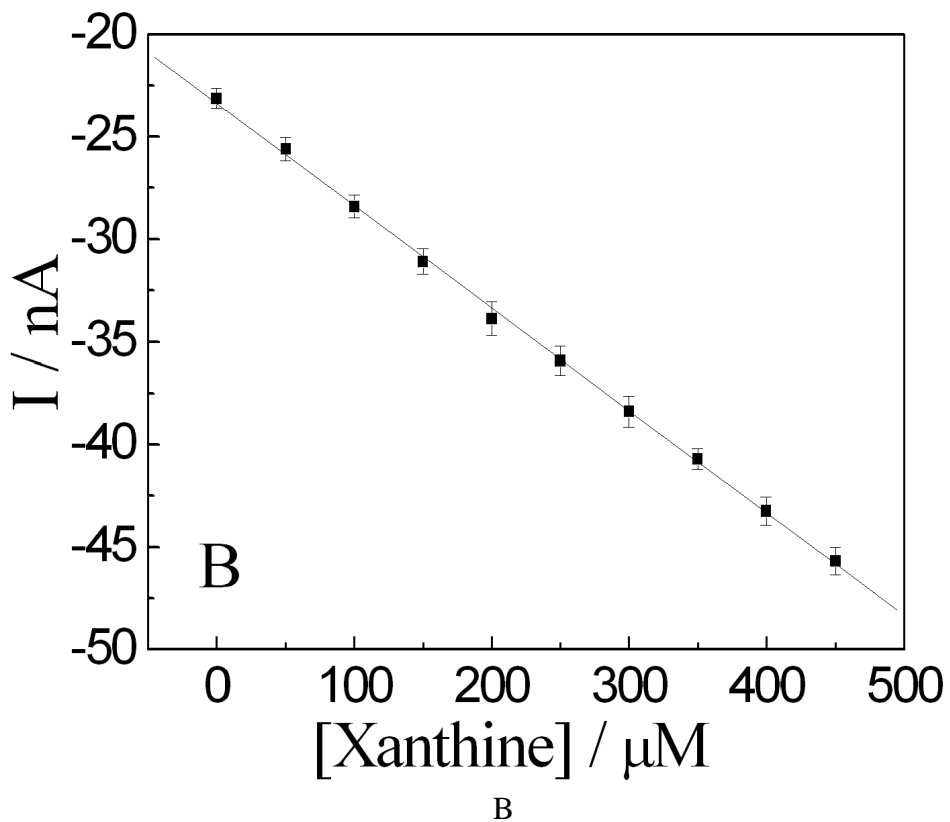
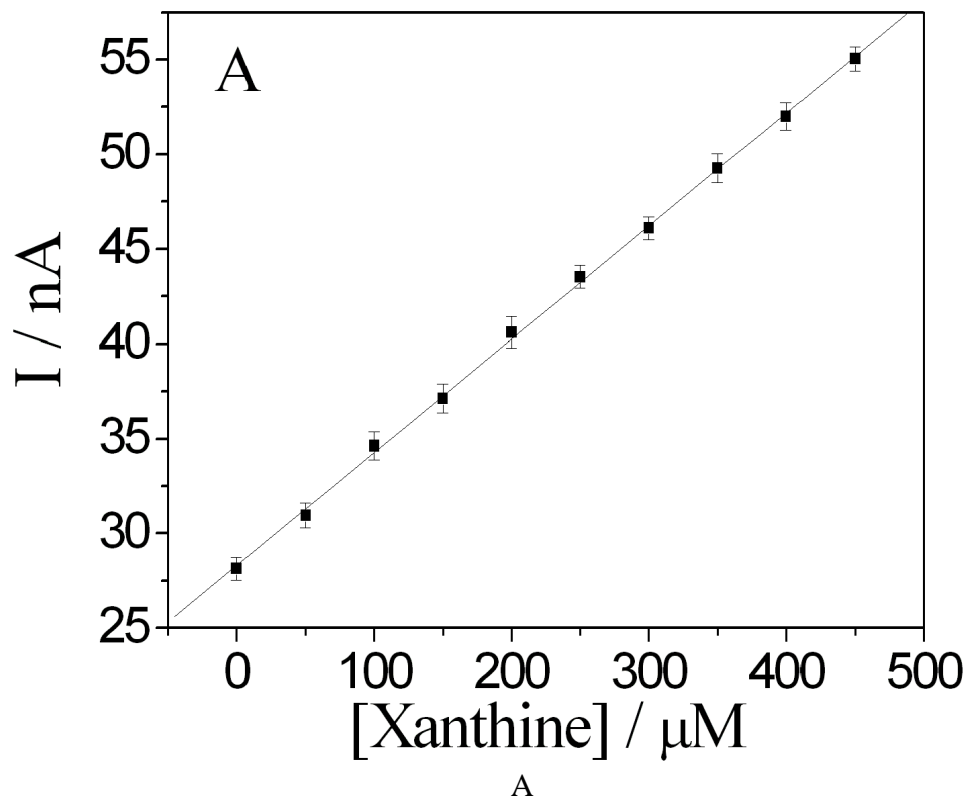


**Figure 6.** Calibration graph of the SOD/ssDNA-GR/BPGE with different xanthine concentrations (0.05–0.45  $\mu\text{M}$ ) at the applied potential of  $-75\text{ mV}$  (A) and  $100\text{ mV}$  (B).

#### 4. CONCLUSIONS

Overall, the remarkably enhanced electron transfer of SOD adsorbed tightly on the surface of ssDNA-GR modified electrode, combined with bidirectional catalytic activity of the SOD toward  $O_2^-$  dismutation essentially allowed us to detect  $O_2^-$  by polarizing the electrode both anodically and cathodically. The advantage of the SOD-based biosensor, together with their good sensing performance and facile-preparation method, sufficiently enables them to be potentially very useful for in vivo and in vitro analysis. Furthermore, these results concerning potential intermediates in SOD will be relevant to future studies of other superoxide-scavenging enzymes as well as oxygen-utilizing copper enzymes where the identities of the reactive oxidants during catalysis are subject to debate.

#### ACKNOWLEDGEMENTS

The authors thank the National Natural Science Foundation of China (20975001), Scientific Research Fund for Young Teachers (2013qnzx55) for fund support.

#### References

1. J.M. McCord, I.J. Fridovich, *J. Biol. Chem.*, 244 (1969) 6049
2. J.A. Tainer, E.D. Getzoff, J.S. Richardson, D.C. Richardson, *Nature*, 306 (1983) 284
3. Y. Tian, T. Ariga, N. Takashima, T. Okajima, L. Mao, T. Ohsaka, *Electrochem. Commun.*, 6 (2004) 609
4. L. Wu, X.H. Zhang, J.H. Chen, *J. Electroanal. Chem.*, 726(2014)1128
5. X. Zhu, X.H. Niu, H.L. Zhao, J. Tang, M.B. Lan, *Biosens. Bioelectron.*, In Press, 2014
6. F. Salem, H. Tavakoli, M. Sadeghi, A. Riazi, *Radiat. Phys. Chem.*, 102 (2014) 128
7. Q. Ye, W. Li, Z. Wang, L.M. Zhang, X.S. Tan, Y. Tian, *J. Electroanal. Chem.*, 729 (2014) 21
8. X.H. Wang, M. Han, J.C. Bao, W.W. Tu, Z.H. Dai, *Anal. Chim. Acta* 717 (2012) 61
9. X.Q. Ji, L. Cui, Y.H. Xu, J.Q. Liu, *Compos. Sci. Technol.*, 106 (2015)25
10. L.B. Ma, X.P. Shen, H. Zhou, Z.Y. Ji, K.M. Chen, G.X. Zhu, *Chem. Eng. J.*, 262 (2015) 980
11. A. Joshi, A. Bajaj, R. Singh, A. Anand, P.S. Alegaonkar, S. Datar, *Compos. Part B: Eng.*, 69 (2015) 472
12. H. D. Jang, S. K. Kim, H. Chang, J.W. Choi, *Biosens. Bioelectron.*, 63 (2015) 546
13. Z.Y. Wang, C.J. Liu, *Nano Energy*, 2015(11) 277
14. K. Inyawilert, A. Wisitsoraat, C. Sriprachaubwong, A. Tuantranont, S. Phanichphant, C. Liewhiran, *Sensor Actuat B-Chem.*, 209 (2015) 40
15. S. Radhakrishnan, K. Krishnamoorthy, C. Sekar, J. Wilson, S. J. Kim, *Chem. Eng. J.*, 259 (2015) 594
16. R. Zacharia, H. Ulbricht, T. Hertel, *Phys. Rev. B* 69 (2004) 155406.
17. H. Teymourian, A. Salimi, S. Firoozi, A. Korani, S. Soltanian, *Electrochim. Acta*, 143 (2014) 196
18. W.M. Si, W. Lei, Z. Han, Y.H. Zhang, Q.L. Hao, M.Z. Xia, *Sensor. Actuat B- Chem.*, 193 (2014)823
19. Z.B. Chen, C.M. Zhang, X.X. Li, H. Ma, C.Q. Wan, K. Li, Y.Q. Lin, *Biosens. Bioelectron.*, 65 (2015) 232
20. W.M. Si, W. Lei, Z. Han, Q.L. Hao, Y.H. Zhang, M.Z. Xia, *Sensor. Actuat. B-Chem.*, 199 (2014) 154
21. D.J. Chung, A.K. Whittaker, S.H. Choi, *J. Appl. Polym. Sci.*, 126(2012) E28
22. A.J. Patil, J.L. Vickery, T.B. Scott, S. Mann, *Adv. Mater.*, 21 (2009) 3159

23. W.S. Hummers, R.E. Offeman, *J. Am. Chem. Soc.*, 80 (1958) 1339
24. E. Laviron, *J. Electroanal. Chem.*, 101 (1979) 19
25. J. Hong, H. Ghourchian, A.A. Moosavi-Movahedi, *Electrochem. Commun.*, 8 (2006) 1572
26. J.A. Fee, P.E. DiCorleto, *Biochem.*, 12 (1973) 4893.
27. E.K. Hodgson, I. Fridovich, *Biochem.* 14 (1975) 5294
28. M.E. McAdam, E.M. Fielden, F. Lavelle, L. Calabrese, D. Cocco, G. Rotilio, *Biochem.*, 167 (1977) 271
29. J.S. Olson, D.P. Ballou, G. Palmer, V. Massey, *J. Biol. Chem.*, 249 (1974) 4350

© 2015 The Authors. Published by ESG ([www.electrochemsci.org](http://www.electrochemsci.org)). This article is an open access article distributed under the terms and conditions of the Creative Commons Attribution license (<http://creativecommons.org/licenses/by/4.0/>).